Ceramics International 50 (2024) 24479–24486

Contents lists available at ScienceDirect

Ceramics International

journal homepage: www.elsevier.com/locate/ceramint

Effects of the addition of slaked lime to alkali-activated pastes based on volcanic ashes from Mt. Etna volcano (Italy)

Claudio Finocchiaro [a], Roberta Occhipinti [a], Germana Barone [a], Paolo Mazzoleni [a,*], Fernanda Andreola [b], Marcello Romagnoli [b], Cristina Leonelli [b]

[a] Department of Biological, Geological and Environmental Sciences, University of Catania, Corso Italia, 57, Catania, 95127, Catania, Italy
[b] Department of Engineering "Enzo Ferrari", University of Modena and Reggio Emilia, Via Pietro Vivarelli 10, 41125, Modena, Italy

ARTICLE INFO

Handling Editor: Dr P. Vincenzini

Keywords:
Volcanic ashes
Rheology
Slaked lime
Setting time
NASH-CASH gel

ABSTRACT

This study provides experimental insights into the optimization of alkali-activated materials (AAMs) carried out in situ at the restoration site of Monreale Cathedral, Italy. Volcanic ash from Mt. Etna volcano (Italy) was used as a precursor to obtain AAMs. Standard and modified pastes with a small amount of slaked lime paste were compared in terms of setting time, rheology, mineralogy, chemical morphology, and mechanical performance. The modified pastes exhibited a faster setting time, superior mechanical strength and rheological properties. Mineralogically, no difference was observed between the two pastes for the small amount of slaked lime paste added very close to the detectable limit (<2 wt%). Moreover, its addition causes slight differences in the morphology of the gel without changing the chemical composition of the Na_2O–CaO–Al_2O_3–SiO_2–H_2O ((N,C)-A-S-H)) type. The results obtained may be useful for the development and optimization of building materials (especially for restoration purposes) where appropriate physico-mechanical performance is required.

1. Introduction

The EU Sustainable Development Goals of Agenda 2030 are driving a rapid shift towards ecological transition and the use of alternative high-performance materials, whose synthesis process does not require thermal treatments, such as the valorisation of natural and/or industrial waste materials [1,2]. These goals focus on sustainability and the circular economy, with the aim of reducing CO_2 emissions and minimize the exploitation of mineral resources [3,4].

In this context, alkali-activated materials (AAMs) offer a greener alternative to traditional cement-based materials, the production of which contributes to approximately 10 % of global CO_2 emissions [5,6]. AAMs are inorganic materials synthesized by mixing a powdered aluminosilicate precursor with an alkaline solution, typically based on NaOH or KOH [7,8]. The solid fraction can be derived from both natural materials and industrial by-products, providing a sustainable solution for waste management [9,10].

Volcanic ash is a potentially exploitable waste material resource for the production of sustainable materials with specific properties suitable for the construction and restoration sectors [11–18]. The chemical and mineralogical compositions of fresh and old volcanic deposits, such as those from Mt. Etna volcano (Italy), confirm their suitability for the alkaline environment required for AAMs [19,20]. Although the latter require the addition of a small amount of metakaolin as an additive to increase the available Al and overcome their low reactivity, previous work has demonstrated their good performance in terms of network reticulation, uniaxial compressive strength, porosity and durability [21,22]. Moreover, the alkaline solution can strongly influence the final performance, with better results observed in potassium-based samples than in sodium-based ones [23]. In addition, volcanic AAMs have shown excellent resistance to atmospheric exposure [24] and salt spray, making them suitable for use in coastal areas [25]. Furthermore, these binders are highly versatile, considering the studies with foaming agents for the production of foamed materials [26] or fire resistance up to 1000 °C [27]. Successful in situ restorations using AAMs have also been carried out, such as the restoration of a mosaic area in the Cathedral of Monreale in Sicily (Italy), a UNESCO World Heritage Site [28].

In order to achieve the above objective, various in situ application tests were carried out to identify the limitations of the standard pastes prepared in the laboratory in order to improve their rheological behaviour for vertical applications. In fact, the standard pastes showed a tendency to drip and did not allow the possibility of engraving for

* Corresponding author.
E-mail address: pmazzol@unict.it (P. Mazzoleni).

https://doi.org/10.1016/j.ceramint.2024.04.181
Received 27 February 2024; Received in revised form 5 April 2024; Accepted 15 April 2024
Available online 16 April 2024

mosaic reproduction. To overcome this challenge, a small amount of CaO-containing additive was incorporated into the paste composition [28].

The processability of AAMs during mixing is often limited by their high viscosity [29]. Consideration of the rheological properties of different AAMs and how to control them can provide valuable guidance for their use in large-scale applications such as pumping, grouting, and 3D printing [30,31]. Literature studies have shown that the addition of lime, namely CaO, to alkali-activated volcanic ash reduces the setting time and slightly increases the compressive strength [32], while the addition of limestone (i.e., $CaCO_3$) develops early strength and Ca-bearing crystalline phases [33]. The alkalinity of the activator solutions plays a crucial role in controlling the dissolution behaviour of the precursor particles, and the adsorption of anionic groups, particularly silicate species, from the activator solution can also influence particle interactions and the rheological behaviour of AAMs [34]. The chemistry of the system can be dramatically altered when Ca-rich precursors are used, resulting in enhanced colloidal interactions between particles [35]. Indeed, the use of the latter complicates the alkali-activation reaction by facilitating the rapid formation of a primary Na_2O–CaO–Al_2O_3–SiO_2–H_2O ((N,C)-A-S-H) gel and a mixed Na_2O–Al_2O_3–SiO_2–H_2O (N-A-S-H) gel [36]. Solid loading and temperature are the most significant variables affecting the rheological behaviour of AAMs, with an increase in solid loading leading to an increase in viscosity and yield stress [37]. This is due to higher interparticle forces in the suspension [38]. Viscosity and yield stress also increase with temperature due to faster geopolymerization reactions. Differences in particle size and reactivity of different precursors and initially precipitated gels can also affect the rheological behaviour. Published literature has shown that AAMs containing NaOH solution have higher yield stress and plastic viscosity than KOH-based mixtures due to the lower charge density of K^+ [39]. Higher NaOH concentration can reduce the yield stress and plastic viscosity, thereby increasing the fluidity of the paste [40]. When combined with reactive $Ca(OH)_2$, an increase in the reaction rate and the compressive strength at early ages and a reduction in the setting time have been shown [41]. However, this behaviour is strongly influenced by the chemical composition of the precursors (e.g., in a high calcium system, the reaction is retarded due to the dilution effect) [42].

This study involved a comparative analysis of standard pastes and pastes that were modified with an additive containing calcium compounds, namely slaked lime, $Ca(OH)_2$ paste. The comparison was carried out using experimental techniques to evaluate both the properties of fresh pastes, namely setting time and rheology, and the microstructure of consolidated samples in terms of mineralogy, morphology and mechanical performance. This work provides experimental insights into the optimization of AAMs carried out in situ at the restoration site of Monreale Cathedral (i.e., UNESCO site) within the completed project "Advanced Green Materials for Cultural Heritage" [28].

2. Materials and methods

2.1. Sample preparation

Pyroclastic deposits collected in the village of Santa Venerina, located on the eastern flank of Mt. Etna volcano (Italy), which erupted in 2013, were used as raw material for this study. Barone et al. [19] recently carried out a chemical and mineralogical analysis of these deposits, revealing a chemical composition of SiO_2 = 49 %; Al_2O_3 = 16 %, Fe_2O_3 = 12 %; TiO_2 = 2 %; Na_2O = 3.5 %; K_2O = 2 %; CaO = 10.5 %; and MgO = 4 %. The main minerals observed in the volcanic products were plagioclase ((Ca–Na)$Al_2Si_2O_8$), augite (Ca(Mg,Fe)Si_2O_6), forsterite ($Mg_2(SiO_4)$) and Fe–Ti-oxides, together with a high proportion of volcanic glass (>60 wt%) [19]. The volcanic ash was washed and dry ground to obtain a grain size <75 μm, suitable for initiating the dissolution reaction in the alkaline environment [43,44]. The activating solution was prepared using sodium hydroxide (8 M), sodium silicate (with a molar ratio of SiO_2/Na_2O = 2) and tap water, to which a commercially available metakaolin, ARGICAL™ M1000 (Imerys, France), was added as a reactive powder. The chemical composition of the latter was found to be SiO_2 = 55 %; Al_2O_3 = 40 %, Fe_2O_3 = 1.4 %; TiO_2 = 1.5 %; $Na_2O + K_2O$ = 0.8 %; CaO + MgO = 0.3 %; and LOI = 1 %. Mineralogically, ARGICAL™ M1000 has been found to consist of quartz (α-SiO_2), anatase (TiO_2), and muscovite ($KAl_2(Si_3Al)O_{10}(OH)_2$) [23].

The rheological tests were carried out on fresh mixtures characterized by the same activating sodium solution, precursors and liquid/solid (L/S) ratios, namely: 80–20 wt% of volcanic ash (V) and metakaolin (M), respectively; water (W) sodium hydroxide (SH) and sodium silicate (SS) ratio, and a liquid to solid ratio (L/S) of 0.32 (Table 1). The manufacturing protocol included the preparation of the activating solution, followed by the addition of the weighted powders, mixing with a mechanical mixer for 5 min, filling of the mold and the application of a vibratory motion to remove air bubbles. A multidisciplinary approach was used to compare the standard and modified pastes, labelled as "ST" and "ST-2SL". In the latter, 2 wt% of slaked lime paste was added to the total mix. The specimens were prepared with dimensions of 8x2x2 cm^3 size and, after 28 days of curing, the mechanical tests were carried out. Their fragments were used for the mineralogical and morphological studies.

2.2. Methods

Various analytical methods were chosen to evaluate the physical properties of the fresh pastes in terms of setting time and rheology, as well as the mineralogical, structural and mechanical properties. The initial and final setting times of the binders were determined using the Vicat test, while rheological analyses were used to estimate viscosity and yield stress. X-ray powder diffraction (XRD) and scanning electron microscopy with energy dispersive X-ray spectroscopy (SEM-EDS) were used to determine the mineralogical composition and the chemical morphological features of the synthetized gels. Finally, flexural and uniaxial compression tests were performed to evaluate the mechanical performance.

2.2.1. Setting time test by the Vicat needle

The setting time of the binder samples was determined using a Vicat apparatus in accordance with AASHTO method [45]. Fresh paste was placed in a standard ring with an internal diameter of 70 mm at the base, 60 mm at the top, and a height of 40 mm. The initial penetration depth was recorded after 1 h, followed by further measurements every 15 min. The initial setting time was determined as the time elapsed between the first contact of the fresh paste and the time when the penetration depth reached 25 mm. The final setting time was determined as the time when the needle no longer penetrated the paste.

2.2.2. Rheological analyses

After preparation, the fresh paste was tested in a rotational controlled stress rheometer (mod. RS100, Haake, Karlsruhe, Germany). For a better evaluation of the rheological behaviour, the instrument was used in: i) Control Rate (CR) mode to determine the flow behaviour and the viscosity curve and ii) Control Stress (CS) mode to determine the yield stress (flow limit). To test the AA pastes, which can be considered as concentrated suspensions, the most suitable sensors are parallel plates of 2 cm in diameter with knurling (PPs20) to minimize slippage. The gap

Table 1
Formulation details of pastes: standard (ST) and modified (ST-2SL) ones. Legend: V = volcanic ash; M = metakaolin; SH = sodium hydroxide; SS = sodium silicate; W = water; L/S = liquid to solid ratio; SL = slaked lime.

Label	V-M (wt%)	SH/SS	W (wt%)	L/S ratio	SL (wt%)
ST	80–20	0.32	5.00	0.32	–
ST-2SL	80–20	0.32	6.00	0.32	2

or distance between the two plates was set at 1.50 mm, which is 5 times larger than the coarsest grain of volcanic ash, i.e., 285 μm. All tests were performed at a constant temperature (20 °C ± 1 °C) maintained by means of a thermostat (mod. DC30, Thermo Fisher, Massachusetts, USA).

2.2.3. X-ray powder diffraction

X-ray powder diffraction (XRPD) measurements were carried out on standard and modified pastes, using a Miniflex Rigaku equipped with a Ni filter and Cu Kα radiation generated at 40 kV and 15 mA. Measurements were made at a scanning speed of 5.0°/min, with a step size of 0.02°, in the 2θ range from 5° to 65°. Qualitative and quantitative data were processed using BGMN/Profex 5.0 software [46], with Rietveld refinement performed by adding a standard corundum powder (NIST code 676a) to each sample at 2 wt% in order to quantify mineralogical phases and amorphous content [47]. The structures of selected phases were identified using the BGMN database (available at http://www.bgmn.de/index.html). The quality of the refinements was assessed based on visual observations of the observed and calculated patterns, as well as the values of discrepancy indices, including the weight profile R-factor, which resulted in values less than 10 % indicating adequate refinement [48].

2.2.4. Scanning electron microscope with EDS

Microanalysis was performed using a Tescan Vega LMU scanning electron microscope (SEM) equipped with an EDAX energy dispersive spectrometer (EDS). Data were collected by focusing the e-beam on the sample at an energy of 20 kV and a beam current of 0.2 nA.

All samples (fragments) were made conductive with a graphite coating. In addition, more detailed information on the distribution of the relevant elements for each sample was obtained by multi-point X-ray analysis.

2.2.5. Mechanical strength

Mechanical tests were performed using a Controls UNIFRAME automatic compression testing machine, with a 10 kN and 50 kN load cell compression for flexure and compression tests, respectively. Three 2x2x8 cm^3 prisms were used for the flexural test and the six half prisms were used as specimens for the uniaxial compressive strength test according to EN 1015-11 standard [49].

3. Results

3.1. Fresh paste characterization: Vicat needle and rheological tests

The results of the Vicat needle setting time test showed a significant difference between the samples tested. Specifically, the modified sample (ST-2SL) showed an initial setting time of 2 h after mixing, followed by hardening after 3 h (final setting time). The standard paste required a longer time of six and a half hours to reach its initial setting time and then hardened after a further one and a half hours (Fig. 1).

The results of the Vicat needle test indicate the time within which the fresh paste can be tested for rheological behaviour prior to induration.

All the samples tested show a non-Newtonian, plastic-like behaviour, as can be seen in Fig. 2, which shows the results of the viscosity versus shear rate for both samples (test run in Control Rate mode). In particular, they show a decrease in viscosity as the velocity gradient increases, with the presence of a yield stress, indicating a plastic behaviour. Observing Fig. 2, the addition of the slaked lime paste at low shear rates ($<30\ s^{-1}$) causes a decrease in the apparent viscosity of the ST-2SL paste. At higher values, the viscosity of both pastes is reversed, although it remains very low. Therefore, the two samples can be considered practically the same, bearing in mind that the values are close to the measuring limits of the instrument.

The yield stress is the critical point at which a material transitions from solid to fluid behaviour as the applied stress increases [50]. This

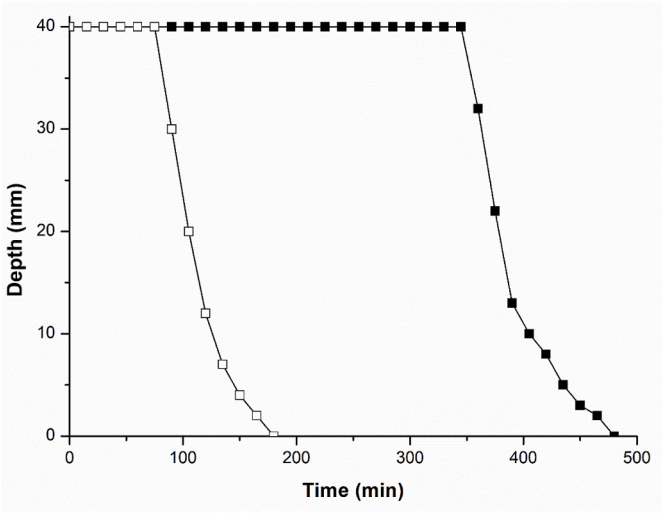

Fig. 1. Trends of setting time test by Vicat needle: (■) ST and (□) ST-2SL pastes.

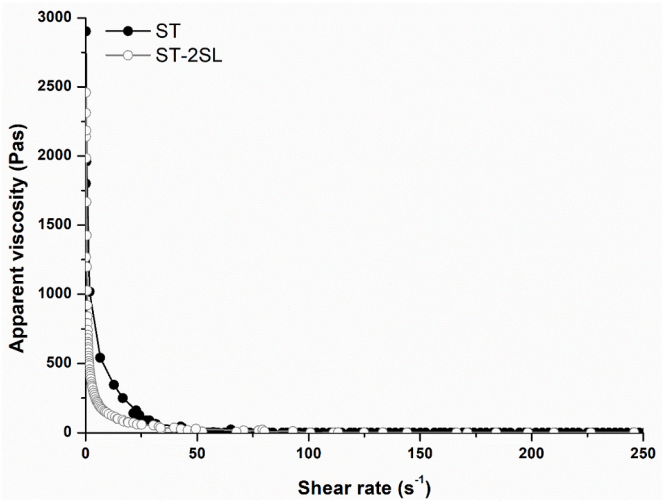

Fig. 2. Apparent viscosity (Pa·s) vs shear rate (s^{-1}) of the standard "ST" and modified "ST-2SL" fresh pastes, tested at 20 °C.

transition occurs when the stress exceeds a certain threshold. In Fig. 3, which shows the stress ramp test performed in Control Stress mode for the ST and ST-2SL samples, we can observe the change in the slope in the curve of deformation (ϒ), the shear strain or shear deformation, which indicates the onset of flow for stresses higher than the yield point. It can also be observed that in the case of the ST sample, the yield stress is around 1100 Pa, while the addition of the slaked lime increases this value to around 2200 Pa (Fig. 3).

It is interesting to note that the addition of 2 wt% of slaked lime paste (SL) to the standard has an obvious effect: it increases the flow limit (yield stress) by more than 100 %.

3.2. Microstructural characterization: mineralogical, chemical and morphological aspects

The mineralogical results of the standard (ST) and modified (ST-2SL) alkali-activated pastes are given in Table 2 and in Fig. 4. Both pastes showed the same mineralogical composition, consisting mainly of plagioclase, augite, olivine, quartz, muscovite and iron hydroxides (hematite and goethite), with a substantial predominance of volcanic amorphous material (Fig. 4a). The modified sample contained a higher

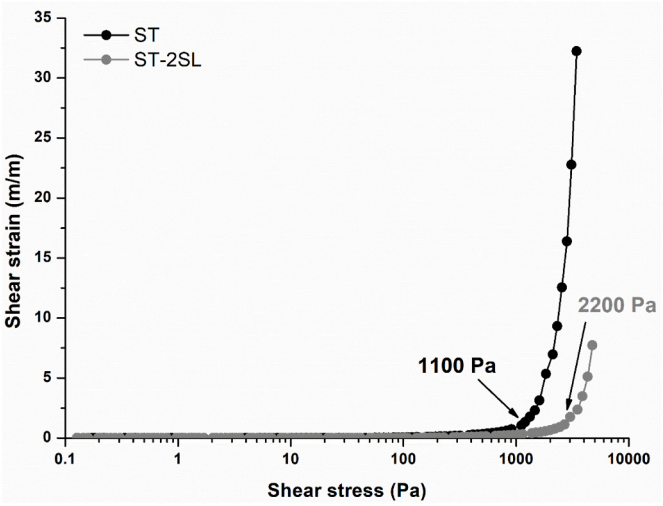

Fig. 3. Shear strain (m/m) vs shear stress (Pa) of the standard "ST" and modified "ST-2SL" fresh pastes, tested at 20 °C for the determination of the yield stress.

Table 2
Mineralogical results (in wt%) obtained by XRD analysis with Rietveld Method. Aug = augite; Fe-ox/hy = hematite and goethite; Ms = muscovite; Ol = olivine; Pl = plagioclase; Qtz = quartz; amorph. = amorphous phase.

	Aug	Fe-ox/hy	Ms	Ol	Pl	Qtz	Amorph.
ST	9	1	1	3	16	1	70
ST-2SL	6	0	1	2	11	1	79

proportion of volcanic amorphous material (79 %) than the standard sample (~70 %) due to the catalytic behaviour of slaked lime on the activation reaction of the mixture [51]. Fig. 4b shows a detail of the XRD pattern of sample ST-2SL, where normally Ca-mineralogical phases appear, allowing a better identification. The main peaks of calcite ($CaCO_3$) and portlandite ($Ca(OH)_2$) (according to the RUFF database: portlandite R070210 and calcite R050128) have been plotted with boxes of 0.4° 2θ width on the pattern. The overlap shows no match with the Ca-phases. Specifically, two boxes do not match any peaks, while the other two, namely one for calcite and one for portlandite, are closer to those of the plagioclase and augite phases at ~18.7° and 29.6° 2θ, respectively. This behaviour may be due to the small amount of slaked lime added to the mixture, which is undetectable due to the detection limit of around 2 wt%, or to the superimposition of more intense diffraction peaks, namely plagioclase and augite, or to their limited diffraction intensity, so that they are confused with background oscillations.

SEM images showing the morphological features at the micrometric scale on the fractured surface of the ST and ST-2SL matrices are shown in Fig. 5. At this scale, the amorphous features of the gel were confirmed. Different morphologies coexist in the same sample, namely unreacted particles, micropores and reaction products (gel). The presence of unreacted particles and crystals typical of the volcanic ash, can be still be seen in both samples.

In detail, the matrix morphology of the ST sample appears to be composed of sub-rounded particles that are partially bonded together, as well as irregular lamellar clusters, due to the presence of metakaolin and its tendency to arrange itself in parallel planes [52,53] (Fig. 5a). The ST-2SL sample shows slight differences in morphology with respect to the ST sample, whose matrix appears more granular and less compact. In addition, the particles in the amorphous matrix are interconnected, forming clusters ending in small acicular fibers (Fig. 5b).

The morphological differences also suggest slight differences in

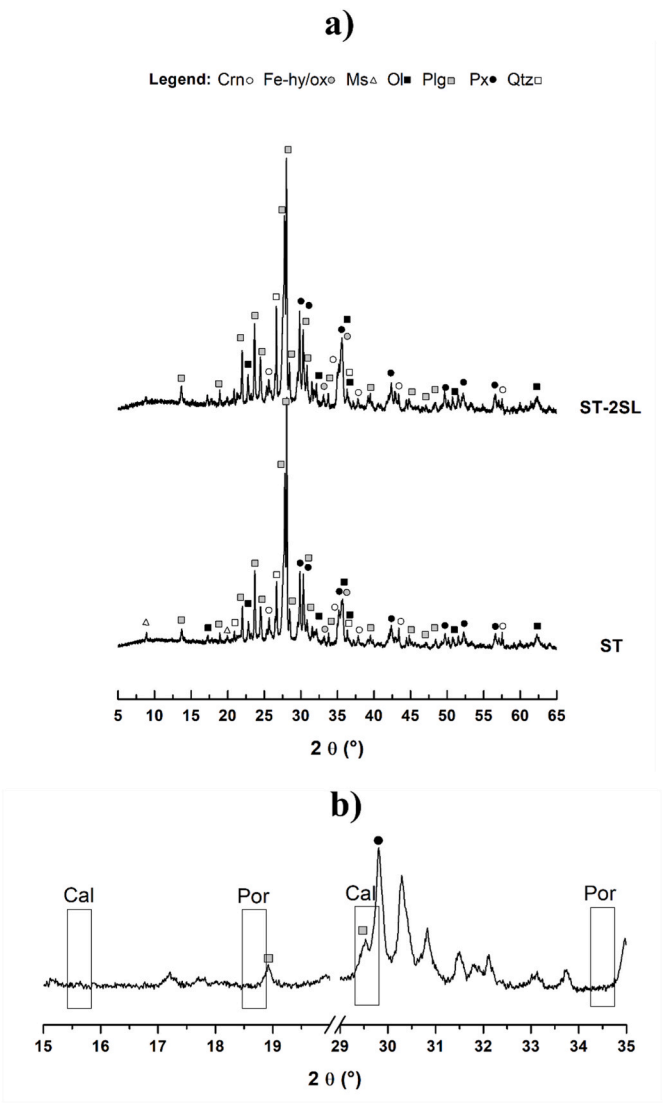

Fig. 4. a) XRD pattern of synthetized pastes; b) focus on the area of ST-2SL sample: the boxes indicate the main peaks of calcite (Cal) and/or portlandite (Por) according to the RRUFF database (https://rruff.info/).

chemical composition as evidenced by EDX analysis (Table 3). Both samples indicate the presence of an aluminosilicate gel with Na_2O, Al_2O_3, SiO_2 and a small amount of CaO in the matrix composition.

In order to better define the composition of the gel phases, the Al_2O_3/SiO_2 and CaO/SiO_2 ratios have been plotted in Fig. 6. The compositional ranges which, according to the literature [54,55], characterize the main types of gels, (C–S–H, C-(A)-S- H, C-A-S-H, N-A-S-H and (N,C)-A-S-H), are also marked on the figure [56].

Both samples are positioned in the N–C-A-S-H gel region, where the small amount of slaked lime added to the ST formulation does not alter the type of gel formed, which is in the N–C-A-S-H region.

3.3. Mechanical performance

Fig. 7 shows the flexural and uniaxial compressive mechanical performance of the specimens tested. The results show a clear variation between the samples. Specifically, the standard paste showed an average uniaxial compressive strength of 24 MPa (σ = 3) and a flexural strength of 7 MPa (σ = 0.6), while the modified paste (ST-2SL) showed a superior average compressive strength of 34 MPa (σ = 3) and a flexural strength of 10 MPa (σ = 1.7). The latter are in agreement with the average

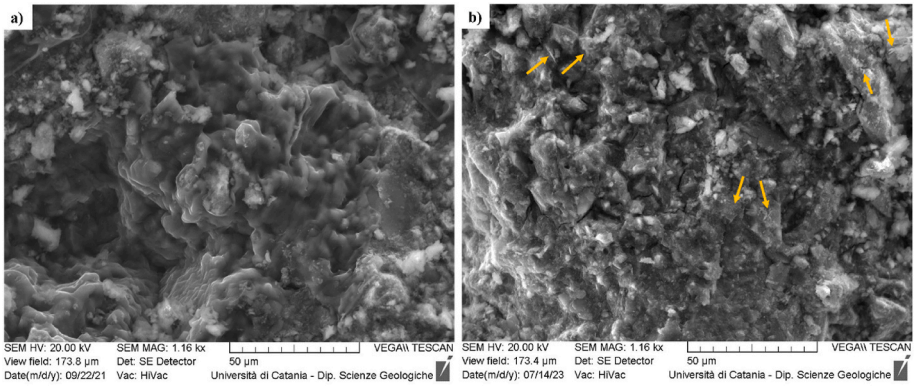

Fig. 5. SEM micrograph of AA-binders: (a) ST and b) ST-2SL samples. The yellow arrows indicate the small acicular fibers. (For interpretation of the references to colour in this figure legend, the reader is referred to the Web version of this article.)

Table 3
Average chemical composition (mean in wt%) and corresponding standard deviation of the matrices based EDX analysis.

	Na_2O	MgO	Al_2O_3	SiO_2	K_2O	CaO	Ti_2O	Fe_2O_3
ST	27.6 ± 0.2	nd	19.3 ± 0.2	43.7 ± 0.3	1.4 ± 0.1	3.1 ± 0.1	1.1 ± 0.1	3.8 ± 0.2
ST-2SL	10.3 ± 0.1	1.4 ± 0.1	22.6 ± 0.2	54.5 ± 0.1	1.5 ± 0.0	5.6 ± 0.1	0.9 ± 0.0	3.2 ± 0.2

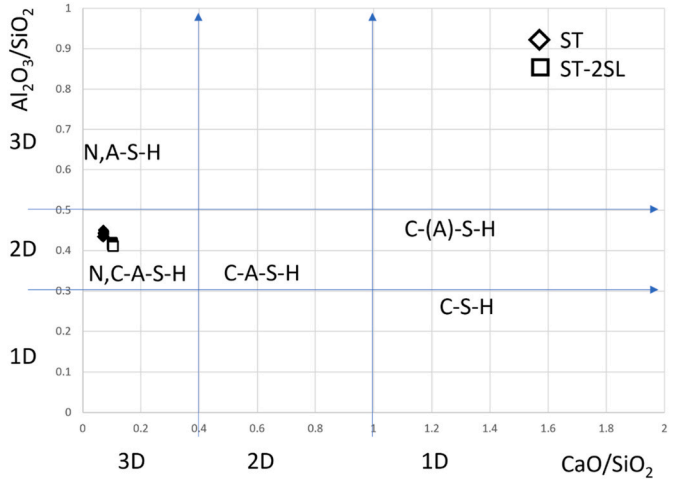

Fig. 6. Al_2O_3/SiO_2 vs. CaO/SiO_2 ratios based on EDX findings for gels of ST and ST-2SL samples [56].

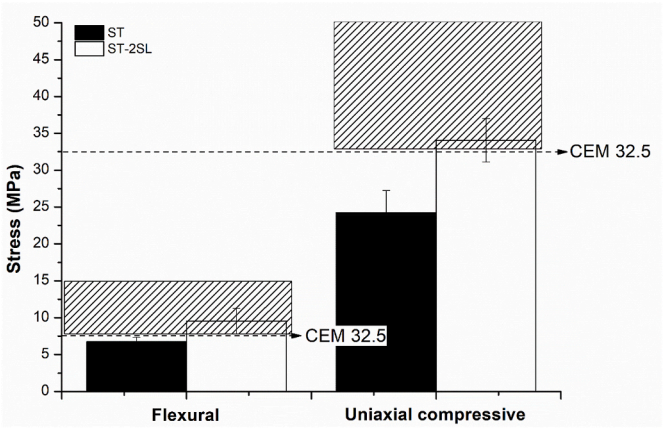

Fig. 7. Histograms of the flexural and uniaxial compressive strength of the specimens tested: ST in black ST and ST-2SL in white. The dashed lines indicate the limit of the average strengths of the CEM 32.5 class, while the dashed boxes the flexural and uniaxial compressive resistance raging values close to the CEM 52.5 class according to the UNI EN 196.1 standard.

strengths of the UNI EN197.1 cement classification [57].

4. Discussion

This work has provided significant insights into various aspects of the effect of incorporating slaked lime into AA paste based on volcanic ash. Vicat tests show a significant reduction in setting time for the modified paste compared to the standard paste. The setting time refers to the period during which the paste changes from a plastic consistency to a solid state. In this case, the modified paste showed a reduction in setting time from six and a half hours to just under 2 h, representing a remarkable 70 % reduction. Reduced setting time can be beneficial in a variety of construction applications where fast construction processes and short project times are required. The reduction in setting time observed with the modified paste can be attributed to the presence of the small amount of slaked lime: this facilitates the acceleration of the paste hydration process, resulting in faster setting times [58,59]. Overall, the results of the Vicat test demonstrate the potential for improved performance in terms of setting times by incorporating a modified paste with a low amount of slaked lime. The increase in yield stress with the addition of 2 wt% of SL results in greater plasticity of the AA paste allowing good application to the wall without undesirable dripping. Moreover, this behaviour may be of interest for other emerging applications, such as the use of AAMs as a building material in 3D printers [60,61]. The addition of SL does not lead to an increase in viscosity which could affect the application. The mineralogical results of both pastes suggest that there is no discernible difference between them, especially for the Ca-phases, possibly due to the low amount of slaked lime added, below the detectable limit [62]. However, the absence of detectable differences in mineralogy does not necessarily mean that the compositions are identical. Depending on the alkalinity of the solution and the nature of the precursors in the mixed system, lower amounts of Ca addition could promote the formation of Ca-rich phases together with the C-A-S-H type of gels [63,64]. In this system, no new Ca-bearing crystalline phases were detected, the main reaction product being a (N,C)-A-S-H gel. The volcanic ash precursor partially releases Ca^{2+} to form an (N,C)-A-S-H reaction product. When slaked lime is added to the mixtures, the

addition of calcium leads to a partial replacement of Na^{+} ions by Ca^{2+} ions without changing the type of gel formed.

The compressive results showed that even a minimal addition of slaked lime resulted in a substantial increase in strength, with an observed increase of at least 30 % in both compressive and flexural strength. This finding suggests that the incorporation of slaked lime promotes the formation of a more durable and robust matrix structure. Indeed, other studies have demonstrated the positive influence of a small amount of Ca-additive on the final physico-mechanical properties in terms of rate and compressive strength of AAMs, although it can significantly reduce the flow of fresh AA paste [65]. Furthermore, its presence can contribute to the overall densification and strengthening of the material, leading to the observed improvements in mechanical properties [66]. The slaked lime can facilitate better bonding between the matrix components, thereby reducing porosity and improving their inter-particle cohesion [67]. This improved bonding may effectively resist crack propagation and improve load transfer mechanisms within the material. However, further investigation is required to fully understand the underlying mechanisms responsible for the observed improvements.

5. Conclusions

On the basis of the satisfactory restoration tests carried out at Cathedral of Monreale (Italy) [28], a multidisciplinary analysis was carried out for the characterization of standard alkali activated paste and the modified one with 2 wt% of slaked lime, based on volcanic ash from Mt. Etna volcano (Italy), revealing interesting physico-mechanical properties. The main conclusions of this study regarding the incorporation of slaked lime are as follows:

- a 70 % reduction in setting time and better rheological properties in the fresh paste;
- the limited addition does not contribute to the formation of Ca-mineralogical phases;
- the small addition of slaked lime causes slight differences in the morphology of the gel, but without changing its chemical composition, the nature of which is (N,C)-A-S-H. No new crystalline Ca-rich phase is formed;
- a more durable structure with a 30 % increase in mechanical performance.

These results have significant implications for the development and optimization of building materials where high physico-mechanical performance is required. However, other properties such as durability and long-term performance should also be assessed to fully evaluate the viability of incorporating slaked lime as a beneficial additive in the production of AA pastes. In addition, the use of specific surfactants will be tested in order to compare the properties with those of the material modified in this work.

Competing interests

The authors declare that they have no known competing financial interests or personal relationships that could have appeared to influence the work reported in this paper.

Data and code availability

Not Applicable.

Ethical approval

Not Applicable.

CRediT authorship contribution statement

Claudio Finocchiaro: Conceptualization, Data curation, Formal analysis, Investigation, Methodology, Writing – original draft, Writing – review & editing. **Roberta Occhipinti:** Conceptualization, Data curation, Formal analysis, Investigation, Methodology, Writing – original draft, Writing – review & editing. **Germana Barone:** Conceptualization, Funding acquisition, Methodology, Project administration, Resources, Supervision, Validation, Visualization, Writing – review & editing. **Paolo Mazzoleni:** Conceptualization, Funding acquisition, Methodology, Project administration, Resources, Supervision, Validation, Writing – review & editing. **Fernanda Andreola:** Conceptualization, Data curation, Formal analysis, Investigation, Methodology, Writing – original draft, Writing – review & editing. **Marcello Romagnoli:** Conceptualization, Data curation, Formal analysis, Investigation, Methodology, Resources, Supervision, Validation, Writing – review & editing. **Cristina Leonelli:** Conceptualization, Data curation, Methodology, Supervision, Validation, Writing – original draft, Writing – review & editing.

Declaration of competing interest

The authors declare that they have no known competing financial interests or personal relationships that could have appeared to influence the work reported in this paper.

Acknowledgements

The group would like to thank to Joseph Cross for his support in syntax revision of the text.

This research was financially supported by the following projects: i) POFESR 2014–2020 entitled "Sicilia Eco Innovative Technologies - SETI", CUP G38I18000960007, funded by “Regione Siciliana” (Sicily, Italy); ii) the EU-funded PON REACT (CUP E65F21002200005) and iii) PNRR PE CHANGE spoke 6 (CUP E63C22001960006) funded by the Italian Ministry of University and Research. However, it has born within the project “Advanced Green Materials for Cultural Heritage” (AGM for CuHe).

References

[1] N.K. Arora, I. Mishra, United nations sustainable development goals 2030 and environmental sustainability: race against time, Environmental Sustainability 2 (4) (2019) 339–342, https://doi.org/10.1007/S42398-019-00092-Y, 2 (2019).
[2] E. Chioatto, P. Sospiro, Transition from waste management to circular economy: the European Union roadmap, Environ. Dev. Sustain. 25 (2023) 249–276, https://doi.org/10.1007/S10668-021-02050-3/FIGURES/6.
[3] J. Brilha, M. Gray, D.I. Pereira, P. Pereira, Geodiversity: an integrative review as a contribution to the sustainable management of the whole of nature, Environ. Sci. Pol. 86 (2018) 19–28, https://doi.org/10.1016/J.ENVSCI.2018.05.001.
[4] I.H. Shah, S.A. Miller, D. Jiang, R.J. Myers, Cement substitution with secondary materials can reduce annual global CO2 emissions by up to 1.3 gigatons, Nat. Commun. 13 (1) (2022) 1–11, https://doi.org/10.1038/s41467-022-33289-7, 13 (2022).
[5] F. Belaïd, How does concrete and cement industry transformation contribute to mitigating climate change challenges? Resources, Conservation & Recycling Advances 15 (2022) 200084 https://doi.org/10.1016/J.RCRADV.2022.200084.
[6] A. Palomo, O. Maltseva, I. Garcia-Lodeiro, A. Fernández-Jiménez, Portland versus alkaline cement: continuity or clean break: “A key decision for global sustainability,”, Front. Chem. 9 (2021) 653, https://doi.org/10.3389/FCHEM.2021.705475/BIBTEX.
[7] F. Pacheco-Torgal, J.A. Labrincha, C. Leonelli, A. Palomo, P. Chindaprasirt, Handbook of Alkali-Activated Cements, Mortars and Concretes, Elsevier Inc., 2014, https://doi.org/10.1016/C2013-0-16511-7.
[8] I. García-lodeiro, A. Palomo, A. Fernández-jiménez, An Overview of the Chemistry of Alkali- Activated Cement-Based Binders, 2015, https://doi.org/10.1533/9781782422884.1.19.
[9] J.L. Provis, Alkali-activated materials, Cement Concr. Res. 114 (2018) 40–48, https://doi.org/10.1016/J.CEMCONRES.2017.02.009.
[10] A. Solouki, G. Viscomi, R. Lamperti, P. Tataranni, Quarry waste as precursors in geopolymers for civil engineering applications: a decade in review, Materials 13 (2020) 3146, https://doi.org/10.3390/MA13143146, 3146 13 (2020).
[11] M. Cavalieri, P.L. Ferrara, C. Finocchiaro, M.F. Martorana, An economic analysis of the use of local natural waste: volcanic ash of Mt. Etna volcano (Italy) for

geopolymer production, Sustainability 16 (2024) 740, https://doi.org/10.3390/SU16020740, 740 16 (2024).
[12] E. Bernardo, H. Elsayed, A. Mazzi, G. Tameni, S. Gazzo, L. Contrafatto, Double-life sustainable construction materials from alkali activation of volcanic ash/discarded glass mixture, Construct. Build. Mater. 359 (2022) 129540, https://doi.org/10.1016/J.CONBUILDMAT.2022.129540.
[13] M.M. Tashima, L. Soriano, M.V. Borrachero, J. Monzó, J. Payá, Towards the valorization of Cumbre Vieja volcanic ash – production of alternative cements, Construct. Build. Mater. 370 (2023) 130635, https://doi.org/10.1016/J.CONBUILDMAT.2023.130635.
[14] P.N. Lemougna, K. tuo Wang, Q. Tang, A.N. Nzeukou, N. Billong, U.C. Melo, X. min Cui, Review on the use of volcanic ashes for engineering applications, Resour. Conserv. Recycl. 137 (2018) 177–190, https://doi.org/10.1016/j.resconrec.2018.05.031.
[15] R. Occhipinti, M.C. Caggiani, L. de Ferri, Z. Xu, C.C. Steindal, N. Razavi, F. Andriulo, P. Mazzoleni, G. Barone, Structural properties of volcanic precursors-based geopolymers before and after natural weathering, Ceram. Int. 49 (2023) 21892–21902, https://doi.org/10.1016/J.CERAMINT.2023.04.013.
[16] S. Tome, D.T. Hermann, V.O. Shikuku, S. Otieno, Synthesis, characterization and application of acid and alkaline activated volcanic ash-based geopolymers for adsorptive remotion of cationic and anionic dyes from water, Ceram. Int. 47 (2021) 20965–20973, https://doi.org/10.1016/J.CERAMINT.2021.04.097.
[17] P.N. Lemougna, K.J.D. MacKenzie, U.F.C. Melo, Synthesis and thermal properties of inorganic polymers (geopolymers) for structural and refractory applications from volcanic ash, Ceram. Int. 37 (2011) 3011–3018, https://doi.org/10.1016/J.CERAMINT.2011.05.002.
[18] P.N. Lemougna, U.F. Chinje Melo, M.P. Delplancke, H. Rahier, Influence of the chemical and mineralogical composition on the reactivity of volcanic ashes during alkali activation, Ceram. Int. 40 (2014) 811–820, https://doi.org/10.1016/j.ceramint.2013.06.072.
[19] G. Barone, C. Finocchiaro, I. Lancellotti, C. Leonelli, P. Mazzoleni, C. Sgarlata, A. Stroscio, Potentiality of the use of pyroclastic volcanic residues in the production of alkali activated material, Waste Biomass Valorization 12 (2021) 1075–1094, https://doi.org/10.1007/s12649-020-01004-6.
[20] G. Lanzafame, M.C. Caggiani, C. Finocchiaro, G. Barone, C. Ferlito, L. Gigli, P. Mazzoleni, Multidisciplinary characterization of the “Ghiara” volcanic paleosoil (Mt. Etna volcano, Italy): petrologic characters and genetic model, Lithos 418–419 (2022) 106679, https://doi.org/10.1016/J.LITHOS.2022.106679.
[21] H. Tchakoute Kouamo, J.A. Mbey, A. Elimbi, B.B. Kenne Diffo, D. Njopwouo, Synthesis of volcanic ash-based geopolymer mortars by fusion method: effects of adding metakaolin to fused volcanic ash, Ceram. Int. 39 (2013) 1613–1621, https://doi.org/10.1016/j.ceramint.2012.08.003.
[22] C. Finocchiaro, G. Barone, P. Mazzoleni, M. Sgarlata, Caterina Lancellotti, Isabella Leonelli, Romagnoli Cristina, Artificial neural networks test for the prediction of chemical stability of pyroclastic deposits-based AAMs and comparison with conventional mathematical approach (MLR), J. Mater. Sci. 56 (2021) 513–527, https://doi.org/10.1007/s10853-020-05250-w.
[23] C. Finocchiaro, G. Barone, P. Mazzoleni, C. Leonelli, A. Gharzouni, S. Rossignol, FT-IR study of early stages of alkali activated materials based on pyroclastic deposits (Mt. Etna, Sicily, Italy) using two different alkaline solutions, Construct. Build. Mater. 262 (2020), https://doi.org/10.1016/j.conbuildmat.2020.120095.
[24] R. Occhipinti, M.C. Caggiani, F. Andriulo, G. Barone, L. de Ferri, P. Mazzoleni, Effect of atmospheric exposure on alkali activated binders and mortars from Mt. Etna volcanic precursors, Mater. Lett. 315 (2022) 131940, https://doi.org/10.1016/j.matlet.2022.131940.
[25] C. Finocchiaro, C.M. Belfiore, G. Barone, P. Mazzoleni, IR-Thermography as a non-destructive tool to derive indirect information on the physical-mechanical behaviour of alkali activated materials, Ceram. Int. (2022), https://doi.org/10.1016/J.CERAMINT.2022.08.174.
[26] R. Occhipinti, G. Lanzafame, A. Lluveras Tenorio, C. Finocchiaro, L. Gigli, M. R. Tinè, P. Mazzoleni, G. Barone, Design of alkali activated foamy binders from Sicilian volcanic precursors, Ceram. Int. (2023), https://doi.org/10.1016/J.CERAMINT.2023.09.220.
[27] P. Scanferla, C. Finocchiaro, A. Gharzouni, G. Barone, P. Mazzoleni, S. Rossignol, High temperature behavior of sodium and potassium volcanic ashes-based alkali-activated materials (Mt. Etna, Italy), Construct. Build. Mater. 408 (2023) 133702, https://doi.org/10.1016/J.CONBUILDMAT.2023.133702.
[28] M. Fugazzotto, R. Occhipinti, M. Cristina Caggiani, A. Coccato, C. Finocchiaro, G. Lanzafame, P. Mazzoleni, G. Nucatolo, G. Piacenti, S. Starinieri, A. Stroscio, G. Barone, Restoration feasibility study by using alkali activated mortars based on Mt. Etna volcanic ash: the case study of Monreale Cathedral (Palermo, Italy), Mater. Lett. 333 (2023) 133626, https://doi.org/10.1016/J.MATLET.2022.133626.
[29] C. Lu, Z. Zhang, C. Shi, N. Li, D. Jiao, Q. Yuan, Rheology of alkali-activated materials: a review, Cem. Concr. Compos. 121 (2021) 104061, https://doi.org/10.1016/J.CEMCONCOMP.2021.104061.
[30] H.S. Gökçe, M. Tuyan, M.L. Nehdi, Alkali-activated and geopolymer materials developed using innovative manufacturing techniques: a critical review, Construct. Build. Mater. 303 (2021) 124483, https://doi.org/10.1016/J.CONBUILDMAT.2021.124483.
[31] H. Güllü, A. Cevik, K.M.A. Al-Ezzi, M.E. Gülsan, On the rheology of using geopolymer for grouting: a comparative study with cement-based grout included fly ash and cold bonded fly ash, Construct. Build. Mater. 196 (2019) 594–610, https://doi.org/10.1016/J.CONBUILDMAT.2018.11.140.
[32] E. Kusumastuti, F.I. Ariati, L. Atmaja, Synthesis of volcanic ash-based geopolymer with calcium oxide (CaO) addition for building material application, J Phys Conf Ser 1567 (2020) 022030, https://doi.org/10.1088/1742-6596/1567/2/022030.
[33] A.A. Adewumi, M.A.M. Ariffin, M. Maslehuddin, M.O. Yusuf, M. Ismail, K.A.A. Al-Sodani, Influence of silica modulus and curing temperature on the strength of alkali-activated volcanic ash and limestone powder mortar, Materials 14 (2021) 5204, https://doi.org/10.3390/MA14185204, 5204 14 (2021).
[34] R.A.A. Boca Santa, J.C. Kessler, C. Soares, H.G. Riella, Microstructural evaluation of initial dissolution of aluminosilicate particles and formation of geopolymer material, Particuology 41 (2018) 101–111, https://doi.org/10.1016/J.PARTIC.2017.12.007.
[35] B. Akturk, A.B. Kizilkanat, N. Kabay, Effect of calcium hydroxide on fresh state behavior of sodium carbonate activated blast furnace slag pastes, Construct. Build. Mater. 212 (2019) 388–399, https://doi.org/10.1016/J.CONBUILDMAT.2019.03.328.
[36] M. Palacios, S. Gismera, M.M. Alonso, J.B. d’Espinose de Lacaillerie, B. Lothenbach, A. Favier, C. Brumaud, F. Puertas, Early reactivity of sodium silicate-activated slag pastes and its impact on rheological properties, Cement Concr. Res. 140 (2021) 106302, https://doi.org/10.1016/J.CEMCONRES.2020.106302.
[37] M. Romagnoli, C. Leonelli, E. Kamse, M. Lassinantti Gualtieri, Rheology of geopolymer by DOE approach, Construct. Build. Mater. 36 (2012) 251–258, https://doi.org/10.1016/j.conbuildmat.2012.04.122.
[38] M. Romagnoli, P. Sassatelli, M. Lassinantti Gualtieri, G. Tari, Rheological characterization of fly ash-based suspensions, Construct. Build. Mater. 65 (2014) 526–534, https://doi.org/10.1016/j.conbuildmat.2014.04.130.
[39] A. Kashani, J.L. Provis, G.G. Qiao, J.S.J. Van Deventer, The interrelationship between surface chemistry and rheology in alkali activated slag paste, Construct. Build. Mater. 65 (2014) 583–591, https://doi.org/10.1016/J.CONBUILDMAT.2014.04.127.
[40] K. Vance, A. Dakhane, G. Sant, N. Neithalath, Observations on the rheological response of alkali activated fly ash suspensions: the role of activator type and concentration, Rheol. Acta 53 (2014) 843–855, https://doi.org/10.1007/S00397-014-0793-Z/FIGURES/12.
[41] X. Dai, S. Aydın, M.Y. Yardımcı, K. Lesage, G. De Schutter, Effect of Ca(OH)2 addition on the engineering properties of sodium sulfate activated slag, Materials 14 (2021), https://doi.org/10.3390/MA14154266.
[42] C. Lin Chan, M. Zhang, Effect of limestone on engineering properties of alkali-activated concrete: a review, Construct. Build. Mater. 362 (2023) 129709, https://doi.org/10.1016/J.CONBUILDMAT.2022.129709.
[43] I. Lancellotti, C. Ponzoni, L. Barbieri, C. Leonelli, Alkali activation processes for incinerator residues management, Waste Manag. 33 (2013) 1740–1749, https://doi.org/10.1016/j.wasman.2013.04.013.
[44] A. Autef, E. Prud’Homme, E. Joussein, G. Gasgnier, S. Pronier, S. Rossignol, Evidence of a gel in geopolymer compounds from pure metakaolin, J. Sol. Gel Sci. Technol. 67 (2013) 534–544, https://doi.org/10.1007/s10971-013-3111-9.
[45] AASHTO, Standard Method of Test for Time of Setting of Hydraulic Cement by Vicat Needle, 2015.
[46] N. Doebelin, R. Kleeberg, Profex: a graphical user interface for the Rietveld refinement program BGMN, J. Appl. Crystallogr. 48 (2015) 1573–1580, https://doi.org/10.1107/S1600576715014685/HTTPS://JOURNALS.IUCR.ORG/SERVICES/RSS.HTML.
[47] A.F. Gualtieri, M. Zanni, Quantitative determination of crystalline and amorphous phase in traditional ceramics by combined rietveld-RIR method, Mater. Sci. Forum 278–281 (1998) 834–839. https://doi.org/10.4028/www.scientific.net/MSF.278-281.834.
[48] D.-C. Nguyen, C.-C. Chu, A.K. Anbalagan, C.-H. Lee, C.-S. Chang, Rietveld refinement and X-ray absorption study on the bonding states of lanthanum-based perovskite-type oxides La1−xCexCoO3, Crystals 12 (2022) 50, https://doi.org/10.3390/CRYST12010050, 50 12 (2021).
[49] EN 1015-11 - Methods of Test for Mortar for Masonry - Part 11: Determination of Flexural and Compressive Strength of Hardened Mortar, 2019.
[50] H.A. Barnes, A Handbook of Elementary Rheology, Inst. of Non Newton…, University of Wales, Aberystwyth, Dyfed, Wales, 2000.
[51] A. Aziz, I.E. El Amrani El Hassani, A. El Khadiri, C. Sadik, A. El Bouari, A. Ballil, A. El Haddar, Effect of slaked lime on the geopolymers synthesis of natural pozzolan from Moroccan Middle Atlas, Journal of the Australian Ceramic Society 56 (2020) 67–78, https://doi.org/10.1007/S41779-019-00361-3.
[52] Y.M. Liew, C.Y. Heah, A.B. Mohd Mustafa, H. Kamarudin, Structure and properties of clay-based geopolymer cements: a review, Prog. Mater. Sci. 83 (2016) 595–629, https://doi.org/10.1016/J.PMATSCI.2016.08.002.
[53] M. Clausi, S.C. Tarantino, L.L. Magnani, M.P. Riccardi, C. Tedeschi, M. Zema, Metakaolin as a precursor of materials for applications in Cultural Heritage: geopolymer-based mortars with ornamental stone aggregates, Appl. Clay Sci. 132–133 (2016) 589–599, https://doi.org/10.1016/j.clay.2016.08.009.
[54] X. Pardal, I. Pochard, A. Nonat, Experimental study of Si–Al substitution in calcium-silicate-hydrate (C-S-H) prepared under equilibrium conditions, Cement Concr. Res. 39 (2009) 637–643, https://doi.org/10.1016/J.CEMCONRES.2009.05.001.
[55] I. Garcia-Lodeiro, A. Palomo, A. Fernández-Jiménez, D.E. MacPhee, Compatibility studies between N-A-S-H and C-A-S-H gels. Study in the ternary diagram Na2O-CaO-Al2O3-SiO 2-H2O, Cement Concr. Res. 41 (2011) 923–931, https://doi.org/10.1016/j.cemconres.2011.05.006.
[56] I. Garcia-Lodeiro, A. Fernández-Jimenez, A. Palomo, Cements with a low clinker content: versatile use of raw materials 4 (2015) 140–151, https://doi.org/10.1080/21650373.2015.1040865.

[57] EN 197-1: Cement - Part 1: Composition, Specifications and Conformity Criteria for Common Cements, 2011.
[58] I. García-Lodeiro, O. Maltseva, Á. Palomo, A. Fernández-Jiménez, Hybrid alkaline cements. Part I: fundamentals, Rev. Rom. Mater./Romanian Journal of Materials 42 (2012) 330–335.
[59] P. Nath, P.K. Sarker, Use of OPC to improve setting and early strength properties of low calcium fly ash geopolymer concrete cured at room temperature, Cem. Concr. Compos. 55 (2015) 205–214, https://doi.org/10.1016/J.CEMCONCOMP.2014.08.008.
[60] H. Zhong, M. Zhang, 3D printing geopolymers: a review, Cem. Concr. Compos. 128 (2022) 104455, https://doi.org/10.1016/J.CEMCONCOMP.2022.104455.
[61] S.H. Bong, M. Xia, B. Nematollahi, C. Shi, Ambient temperature cured 'just-add-water' geopolymer for 3D concrete printing applications, Cem. Concr. Compos. 121 (2021) 104060, https://doi.org/10.1016/J.CEMCONCOMP.2021.104060.
[62] A. Ali, Y.W. Chiang, R.M. Santos, X-Ray diffraction techniques for mineral characterization: a review for engineers of the fundamentals, applications, and research directions, Minerals 12 (2022) 205, https://doi.org/10.3390/MIN12020205, 205 12 (2022).
[63] R. Occhipinti, A.M. Fernández-Jiménez, A. Palomo, S.C. Tarantino, M. Zema, Sulfate-bearing clay and Pietra Serena sludge: raw materials for the development of alkali activated binders, Construct. Build. Mater. 301 (2021) 124030, https://doi.org/10.1016/J.CONBUILDMAT.2021.124030.
[64] A.A. Adewumi, M.A.M. Ariffin, M.O. Yusuf, M. Maslehuddin, M. Ismail, Effect of sodium hydroxide concentration on strength and microstructure of alkali-activated natural pozzolan and limestone powder mortar, Construct. Build. Mater. 271 (2021) 121530, https://doi.org/10.1016/J.CONBUILDMAT.2020.121530.
[65] S. Park, K.A. Moges, S. Wu, S. Pyo, Characteristics of hybrid alkaline cement composites with high cement content: flash set and high compressive strength, J. Mater. Res. Technol. 17 (2022) 1582–1597, https://doi.org/10.1016/J.JMRT.2022.01.105.
[66] B. Balun, M. Karata, Compressive Strength of Pumice Based Alkali-Activated Hybrid Cement Compressive Strength of Pumice Based Alkali-Activated Hybrid Cement, 2018.
[67] M.H. Raza, M. Khan, R.Y. Zhong, Strength, porosity and life cycle analysis of geopolymer and hybrid cement mortars for sustainable construction, Sci. Total Environ. 907 (2024) 167839, https://doi.org/10.1016/J.SCITOTENV.2023.167839.